

# Manual and Computer-Assisted Pedicle Screw Placement Plans: A Quantitative Comparison

Dejan Knez<sup>1</sup>(✉), Janez Mohar<sup>2</sup>, Robert J. Cirman<sup>2</sup>, Boštjan Likar<sup>1</sup>,  
Franjo Pernuš<sup>1</sup>, and Tomaž Vrtovec<sup>1</sup>

<sup>1</sup> Faculty of Electrical Engineering, University of Ljubljana, Ljubljana, Slovenia  
{dejan.knez,bostjan.likar,franjo.pernus,tomaz.vrtovec}@fe.uni-lj.si

<sup>2</sup> Valdoltra Orthopaedic Hospital, Ankaran, Slovenia  
{janez.mohar,robertjanez.cirman}@ob-valdoltra.si

**Abstract.** In this paper, we present a quantitative comparison of manual and computer-assisted preoperative pedicle screw placement plans, obtained from three-dimensional (3D) computed tomography (CT) images of 17 patients with thoracic spinal deformities. Manual planning was performed by two spine surgeons by means of a dedicated software for planning of surgical procedures, while computer-assisted planning was based on automated 3D segmentation and modeling of vertebral structures from CT images, and automated modeling of the pedicle screw in 3D with maximization of the screw fastening strength. The analysis of the size (diameter and length) and insertion trajectory (pedicle crossing point, sagittal and axial inclinations) for 316 pedicle screws revealed a statistically significant difference in the screw size and insertion trajectory. However, computer-assisted planning did not propose narrower and shorter screws, which was reflected through a higher normalized screw fastening strength.

## 1 Introduction

Vertebral fixation by pedicle screw placement is one of the most widely used stabilization techniques in spine surgery [1–3]. It is used for treating various pathological conditions of the spine, such as deformities, tumors and fractures, as well as for other degenerations that cause spinal instability. The procedure is based on anchoring two (or more) vertebrae to each other by inserting screws through vertebral pedicles from the posterior side so that they reach the interior of the vertebral body, and then bilaterally (i.e. on each side of the vertebra) attaching a stabilizing rod to the exterior part of the screws [4]. As such, the procedure is considered complex and technically demanding with a steep learning curve, because the visibility of anatomical structures is limited during the surgery, and therefore a mental conceptualization of three-dimensional (3D) spinal anatomical structures that are hidden from direct view is required.

Although pedicles are, from the biomechanical point of view, the hardest part of the vertebra, their narrow anatomical shape poses a risk of injury to the spinal cord, spinal nerve roots, vascular structures and vital organs that can

be caused by pedicle wall breakthrough or other damage in the case of pedicle screw misplacement [5]. For a safe pedicle screw placement, the spine surgeon has to perform proper surgery planning by taking into account the morphometry (shape and structure) of pedicles and vertebral bodies, and choosing the appropriate size (i.e. diameter and length) and insertion trajectory (i.e. entry point and inclinations) of each pedicle screw, which has proved valuable for reducing the risk of screw misplacement. However, the accuracy of pedicle screw placement is directly related to the expertise of the spine surgeon, and therefore several methods for computer-assisted surgery (CAS) have been developed, where intraoperative navigation based on markers and adequate software is used to visualize and track surgical instruments relative to the patient anatomy [6]. The advantages of CAS are reflected in a less invasive surgery, higher accuracy of pedicle screw placement, lower costs from the point of view of screw misplacement, and in allowing simulations, which help spine surgeons to gain experience. On the other hand, the disadvantages of CAS are variable patient positioning during the procedure, variable accuracy of surgical instrument tracking and a relatively high cost of the system.

Preoperative surgery planning based on 3D images of the spine, which are usually acquired by the computed tomography (CT) imaging technique [7] that provides an accurate insight into the anatomical structure and shape of the spine, has become essential for pedicle screw placement. In this paper, we present a quantitative comparison of manual and computer-assisted pedicle screw placement plans, obtained from CT images with thoracic spinal deformities.

## 2 Methodology

### 2.1 Manual Pedicle Screw Placement Plans

Manual planning was performed by means of 3D visualization of the spine anatomy from CT images and by using a dedicated medical software for trauma and orthopedic surgery planning (EBS, Ekliptik d.o.o., Ljubljana, Slovenia), which was divided into three steps. In the first step, the spine was segmented by simple thresholding of CT image intensities to obtain the corresponding 3D triangular mesh model, which enabled 3D visualization of the spine (Fig. 1(a)). In the second step, manual labeling of vertebrae (segments T1–T12) was first performed based on the visualized 3D spine model and the CT image, and then the initial pedicle screw insertion trajectory was determined by placing a 3D pedicle screw model into the 3D spine model and the CT image, and through its manipulation the virtual screw entry point into each observed pedicle and the virtual screw exit point from the corresponding vertebral body were identified (Fig. 1(b)). The final pedicle screw trajectory (i.e. entry point and inclinations) was determined in the third step by moving the pedicle screw virtual entry and exit points within the oblique cross-section, defined by the initial insertion trajectory and the normal to the current view in the 3D space (Fig. 1(c)), while the final pedicle screw size (i.e. diameter and length) was determined by a thorough analysis of the anatomy of the observed pedicle and the corresponding vertebral

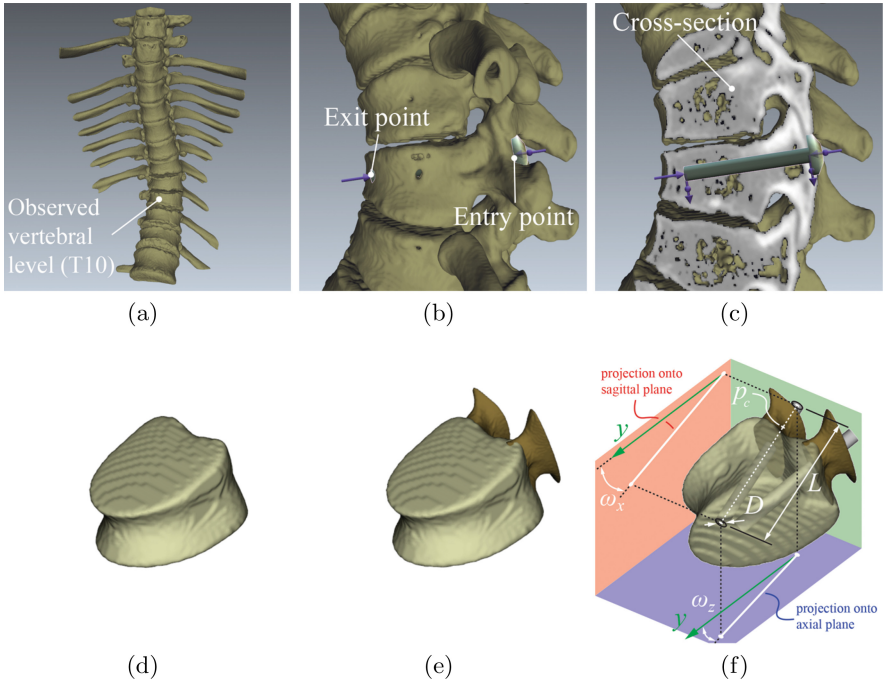


**Fig. 1.** Manual ((a)–(c)) and computer-assisted ((d)–(f)) planning of the pedicle screw size and insertion trajectory. (a) The 3D triangular mesh model of the spine, obtained by thresholding the CT image. (b) Determination of the virtual entry point into the pedicle and the virtual exit point from the vertebral body. (c) Determination of the final pedicle screw trajectory within the predefined cross-section. (d) The 3D model of the vertebral body, representing its segmentation from the CT image. (e) The 3D models of the left and right pedicle, representing their segmentations from the CT image. (f) The 3D models of the screws through the left and right pedicle.

body. The resulting pedicle screw sizes and insertion trajectories had to provide a high level of safety for their insertion (i.e. preventing pedicle and/or vertebral body wall breakthrough) considering the maximal allowable screw diameters and lengths, which were consistent with the usage and availability of pedicle screws in clinical practice, i.e. the screw diameter was determined by increments of 0.5 mm and the screw length by increments of 5 mm. In the case the pedicle anatomy did not allow a safe insertion of the screw with a diameter of at least 3 mm (the smallest available diameter), the screw was excluded from the preoperative plan.

## 2.2 Computer-Assisted Pedicle Screw Placement Plans

Computer-assisted planning was performed by means of the method proposed by Knez et al. [8] that first automatically segments the vertebral bodies and pedicles from the CT image by 3D geometrical modeling, and then automatically

determines the size and insertion trajectory of each pedicle screw by modeling the screw in 3D and maximization of its fastening strength.

The initial 3D vertebral body model is represented in the form of an elliptical cylinder, which is then deformed by introducing additional shape parameters and aligned to the observed vertebral body in the CT image by maximizing the similarity between the 3D model and the corresponding anatomy. The final 3D vertebral body model (Fig. 1(d)) is represented by 31 parameters, out of which six represent its position and orientation in the 3D image, three represent its 3D size and the remaining 22 represent specific 3D anatomical deformations of the vertebral body (i.e. the shape of the vertebral body at the location of the left pedicle, right pedicle, vertebral foramen and anterior part of the vertebral body; the concavity of the vertebral body wall at its anterior part and at the vertebral foramen; the concavity and sagittal inclinations of vertebral endplates; the increasing size and torsion of the vertebral body).

The obtained final 3D vertebral body model is used to define the location of the initial 3D pedicle model, which is also represented in the form of an elliptical cylinder, and is then again deformed by introducing additional shape parameters and aligned to the observed pedicle in the CT image. The final 3D pedicle model (Fig. 1(e)) is represented by 38 parameters, out of which six represent its position and orientation in the 3D image, three represent its 3D size and the remaining 29 represent specific 3D anatomical deformations of the pedicle (i.e. the pedicle wall concavity at its anterior, posterior, right and left parts; the shape of the pedicle at its anterior, posterior, right and left tails; the teardrop and kidney shape of the pedicle cross-section; the torsion of the pedicle).

Both the obtained final 3D vertebral body and pedicle models are then used to model the corresponding pedicle screw in the form of a circular cylinder (Fig. 1(f)). The pedicle screw size (i.e. diameter and length) is determined from the geometrical properties of the corresponding anatomy, represented by the 3D vertebral body and pedicle models, i.e. its diameter is determined as 70% of the narrowest pedicle diameter [9], while its length as 80% of the anteroposterior size of the vertebral body [2]. On the other hand, the pedicle screw insertion trajectory (i.e. entry point and inclination angles) is determined from the structural properties of the corresponding anatomy by maximizing the screw fastening strength, defined as the sum of the underlying CT image intensities. It was shown that CT image intensities as well as the screw pull-out strength correlate with the corresponding bone mineral density (BMD) [2,10], and consequently the screw fastening strength is strongly related with its pull-out strength [11], which represents one of the most important biomechanical properties for pedicle screw placement. For the computation of the fastening strength, only CT image intensities within a relatively small neighborhood of the 3D pedicle screw surface, representing the surrounding volume around the screw thread, are taken into account and additionally weighted according to the distance from the longitudinal pedicle axis in order to reduce the potential impact of higher intensities close to the pedicle screw surface. Moreover, the fastening strength is normalized with the surrounding volume around the screw thread to avoid the influence of different

**Table 1.** The number of the observed vertebral bodies (VBs) and pedicle screws for each vertebral segment (T1–T12) and patient’s diagnosis, i.e. adolescent idiopathic scoliosis (AIS) and Scheuermann’s kyphosis (SK) in CT images of the thoracic spine from 17 patients.

Segment	T1	T2	T3	T4	T5	T6	T7	T8	T9	T10	T11	T12	All
No. of VBs	3	10	12	13	14	15	14	17	16	17	17	16	<b>164</b>
AIS	3	8	10	11	11	12	11	13	13	13	13	12	<b>130</b>
SK	0	2	2	2	3	3	3	4	3	4	4	4	<b>34</b>
No. of screws	6	20	22	23	27	28	27	33	31	33	34	32	<b>316</b>
AIS	6	16	19	19	22	22	21	25	25	26	26	24	<b>250</b>
SK	0	4	3	4	5	6	6	8	6	8	8	8	<b>66</b>

screw sizes. Besides structural, also geometrical properties of the corresponding anatomy are taken into account for the determination of the pedicle screw insertion trajectory, i.e. each screw has to be completely inside the corresponding 3D vertebral body and pedicle models, and the intersection point between the screw insertion trajectory and the plane of sagittal symmetry of the vertebral body has to be outside the corresponding 3D vertebral body model. Therefore, computer-assisted planning automatically determines the optimal pedicle screw size and insertion trajectory with the highest possible screw fastening strength according to the structure of the observed vertebra while limiting both the screw size and insertion trajectory by the anatomical shape of the observed pedicle and the corresponding vertebral body.

### 3 Results

Quantitative comparison of pedicle screw placement plans was performed for 17 patients (males: 12; females: 5; mean age: 17.6 years; age range: 12–14 years) with thoracic spinal deformities (adolescent idiopathic scoliosis: 13; Scheuermann’s kyphosis: 4). All patients were appointed for the pedicle screw placement surgery at Orthopaedic Hospital Valdoltra, Slovenia, between 2013 and 2016. For the purpose of surgery planning, preoperative CT images of the thoracic spine were acquired, usually between the first (T1) and last (T12) thoracic vertebra (GE LightSpeed VTC; pixel size: 0.25–0.38 mm; slice thickness: 0.6 mm). For all patients, a spine surgeon manually defined preoperative pedicle screw placement plans that were used to construct patient-specific drill guides, which were intraoperatively laid over the visible part of the spine. Pedicle screws with pre-defined sizes were then placed along these guides, which defined their insertion trajectory.

For the purpose of quantitative comparison, manual planning was additionally performed by two experienced spine surgeons, who independently determined pedicle screw sizes and insertion trajectories as described in Sect. 2.1 (first surgeon:  $M_1$ ; second surgeon:  $M_2$ ), while computer-assisted planning was

performed by the automated method of Knez et al. [8] as described in Sect. 2.2 (computer: C) with an estimated modeling accuracy of  $0.39 \pm 0.31$  mm for vertebral bodies and  $0.31 \pm 0.25$  mm for pedicles [8] in terms of the mean absolute difference (MAD) and corresponding standard deviation (SD). The results were obtained for CT images of all 17 patients, where the parameters for 316 pedicle screws through 158 left and 158 right pedicles of 164 vertebral bodies were determined (Table 1). The obtained pedicle screw parameters consisted of the screw size (i.e. diameter  $D$  and length  $L$ ), insertion trajectory (i.e. pedicle crossing point  $p_c = [x_c, y_c, z_c]$ , sagittal  $\omega_x$  and axial  $\omega_z$  inclinations) and normalized fastening strength  $F_n$  (Fig. 1(f)). For each parameter of the pedicle screw, three values ( $M_1$ ,  $M_2$  and C) were independently obtained and further used for quantitative comparison and statistical analysis (Student  $t$ -test; significance level:  $p < 0.05$ ). The results are presented in Tables 2 and 3, while Fig. 2 shows examples of the obtained pedicle screw placement plans.

The quantitative comparison of the obtained pedicle screw sizes and insertion trajectories between manual plans  $M_1$  and manual plans  $M_2$  (Tables 2 and 3)

**Table 2.** Quantitative comparison of manual ( $M_1$  and  $M_2$ ) and computer-assisted (C) preoperative planning of the size (i.e. diameter  $D$  and length  $L$ ) and insertion trajectory (i.e. pedicle crossing point  $p_c$ , sagittal inclination angle  $\omega_x$  and axial inclination angle  $\omega_z$ ) for 316 pedicle screws in CT images of the thoracic spine (segments T1–T12) from 17 patients in terms of the mean absolute difference (MAD) and corresponding standard deviation (SD).

Segment	T1	T2	T3	T4	T5	T6	T7	T8	T9	T10	T11	T12	All
$D\{M_1 \text{ vs. } M_2\}$ (mm)	0.8 (0.5)	0.5 (0.5)	0.3 (0.3)	0.2 (0.2)	0.3 (0.4)	0.3 (0.4)	0.3 (0.3)	0.6 (0.5)	0.5 (0.4)	0.6 (0.5)	0.4 (0.4)	0.4 (0.4)	<b>0.4</b> <b>(0.4)</b>
$D\{M_1 \text{ vs. } C\}$ (mm)	1.0 (0.7)	0.6 (0.5)	0.3 (0.4)	0.4 (0.4)	0.3 (0.4)	0.4 (0.5)	0.3 (0.4)	0.6 (0.6)	0.4 (0.4)	0.7 (0.6)	0.8 (0.5)	0.6 (0.4)	<b>0.5</b> <b>(0.5)</b>
$D\{M_2 \text{ vs. } C\}$ (mm)	0.4 (0.4)	0.3 (0.3)	0.4 (0.3)	0.4 (0.3)	0.4 (0.3)	0.4 (0.3)	0.4 (0.4)	0.4 (0.3)	0.4 (0.3)	0.3 (0.3)	0.5 (0.4)	0.5 (0.4)	<b>0.4</b> <b>(0.3)</b>
$L\{M_1 \text{ vs. } M_2\}$ (mm)	1.7 (2.6)	3.0 (3.0)	2.5 (2.6)	3.0 (2.9)	2.0 (3.2)	2.5 (2.5)	2.6 (3.2)	2.8 (2.8)	3.4 (3.3)	2.7 (2.5)	2.6 (3.3)	4.2 (3.4)	<b>2.9</b> <b>(3.0)</b>
$L\{M_1 \text{ vs. } C\}$ (mm)	2.3 (1.9)	3.2 (2.4)	3.7 (2.5)	4.1 (3.2)	2.7 (2.1)	3.4 (4.0)	4.3 (3.9)	4.1 (3.7)	4.5 (3.7)	3.8 (3.5)	3.5 (2.6)	6.7 (3.8)	<b>4.0</b> <b>(3.4)</b>
$L\{M_2 \text{ vs. } C\}$ (mm)	2.0 (1.8)	2.3 (1.5)	4.0 (4.4)	3.3 (3.2)	2.4 (1.5)	3.3 (3.1)	3.0 (2.3)	3.0 (4.0)	4.3 (4.1)	3.7 (3.4)	3.6 (3.0)	5.0 (3.3)	<b>3.5</b> <b>(3.3)</b>
$p_c\{M_1 \text{ vs. } M_2\}$ (mm)	1.2 (0.9)	1.3 (1.0)	0.3 (0.7)	1.4 (0.9)	1.3 (1.0)	1.4 (1.0)	1.4 (1.4)	1.4 (1.1)	1.4 (1.2)	2.0 (1.6)	2.8 (2.2)	2.0 (1.2)	<b>1.7</b> <b>(1.4)</b>
$p_c\{M_1 \text{ vs. } C\}$ (mm)	2.0 (1.1)	1.3 (1.1)	1.5 (1.0)	1.3 (1.0)	1.1 (0.8)	1.2 (0.9)	1.2 (0.9)	1.5 (1.2)	1.4 (0.8)	1.6 (0.9)	2.3 (1.3)	2.1 (1.1)	<b>1.6</b> <b>(1.1)</b>
$p_c\{M_2 \text{ vs. } C\}$ (mm)	1.4 (1.2)	1.3 (1.1)	1.1 (0.7)	1.0 (0.6)	1.3 (1.0)	1.3 (0.7)	1.3 (0.7)	1.4 (0.9)	1.4 (0.9)	1.9 (1.5)	2.1 (1.2)	1.9 (1.4)	<b>1.5</b> <b>(1.1)</b>
$\omega_x\{M_1 \text{ vs. } M_2\}$ ( $^\circ$ )	5.3 (2.8)	3.6 (2.9)	3.1 (3.3)	3.9 (3.4)	4.1 (3.3)	3.7 (3.2)	4.3 (3.2)	3.5 (2.8)	3.3 (2.8)	3.7 (2.7)	5.0 (3.7)	3.7 (3.4)	<b>3.8</b> <b>(3.2)</b>
$\omega_x\{M_1 \text{ vs. } C\}$ ( $^\circ$ )	18.6 (7.4)	7.7 (6.8)	8.5 (4.0)	8.4 (5.6)	11.3 (6.0)	9.7 (5.9)	10.3 (5.8)	10.5 (4.5)	10.7 (5.7)	12.1 (5.4)	11.7 (6.6)	9.7 (5.9)	<b>10.4</b> <b>(5.9)</b>
$\omega_x\{M_2 \text{ vs. } C\}$ ( $^\circ$ )	17.1 (4.3)	7.6 (4.7)	8.6 (3.8)	8.0 (4.4)	10.1 (5.4)	10.1 (6.0)	10.8 (4.8)	10.3 (4.3)	10.2 (6.3)	12.0 (6.0)	13.5 (7.8)	8.9 (5.5)	<b>10.6</b> <b>(5.9)</b>
$\omega_z\{M_1 \text{ vs. } M_2\}$ ( $^\circ$ )	3.7 (2.4)	6.9 (3.4)	5.3 (3.4)	3.2 (2.8)	3.7 (2.8)	3.7 (2.9)	4.7 (3.5)	4.3 (3.0)	4.5 (2.8)	4.1 (3.1)	4.0 (3.3)	3.2 (3.0)	<b>4.2</b> <b>(3.3)</b>
$\omega_z\{M_1 \text{ vs. } C\}$ ( $^\circ$ )	2.9 (3.0)	7.9 (5.0)	5.6 (3.9)	4.2 (3.0)	4.9 (4.4)	5.3 (3.6)	5.8 (4.5)	5.9 (4.2)	6.1 (3.5)	6.4 (4.0)	5.6 (4.1)	6.2 (4.6)	<b>5.8</b> <b>(4.1)</b>
$\omega_z\{M_2 \text{ vs. } C\}$ ( $^\circ$ )	4.0 (3.1)	3.8 (2.9)	4.4 (4.6)	4.1 (2.6)	4.2 (3.1)	4.2 (2.8)	4.7 (3.6)	4.4 (3.0)	4.0 (2.6)	5.0 (3.8)	5.2 (4.3)	5.8 (5.1)	<b>4.6</b> <b>(3.6)</b>

**Table 3.** Quantitative comparison of manual ( $M_1$  and  $M_2$ ) and computer-assisted ( $C$ ) preoperative planning of the normalized fastening strength  $F_n$  for 316 pedicle screws in CT images of the thoracic spine (segments T1–T12) from 17 patients in terms of the mean absolute difference (MAD) and corresponding standard deviation (SD).

Segment	T1	T2	T3	T4	T5	T6	T7	T8	T9	T10	T11	T12	All
$F_n\{M_1 \text{ vs. } M_2\}$ (%)	47 (5)	19 (25)	16 (22)	12 (19)	12 (12)	11 (16)	10 (8)	8 (6)	8 (7)	8 (10)	10 (6)	12 (16)	<b>11</b> <b>(14)</b>
$F_n\{M_1 \text{ vs. } C\}$ (%)	11 (10)	26 (36)	12 (14)	18 (32)	13 (12)	14 (9)	15 (15)	18 (17)	17 (19)	18 (23)	15 (15)	15 (16)	<b>16</b> <b>(20)</b>
$F_n\{M_2 \text{ vs. } C\}$ (%)	12 (9)	22 (44)	14 (21)	24 (30)	21 (19)	20 (23)	21 (16)	20 (19)	10 (16)	18 (21)	16 (12)	16 (15)	<b>19</b> <b>(22)</b>

revealed that the differences between  $M_1$  and  $M_2$  are on average  $0.4 \pm 0.4$  mm for diameter  $D$  and  $2.9 \pm 3.0$  mm for length  $L$  related to the pedicle screw size,  $1.7 \pm 1.4$  mm for pedicle crossing point  $p_c$ ,  $3.8 \pm 3.2^\circ$  for sagittal inclination  $\omega_x$  and  $4.3 \pm 3.3^\circ$  for axial inclination  $\omega_z$  related to the insertion trajectory, and  $11 \pm 14\%$  for normalized screw fastening strength  $F_n$ . Statistically significant differences were observed for planning of the pedicle screw size ( $p < 0.001$ ) and inclinations ( $p < 0.05$ ), where, in comparison to  $M_2$ , manual planning  $M_1$  proposed narrower ( $p < 0.05$ ) and longer ( $p < 0.05$ ) screws with a smaller corresponding normalized fastening strength ( $p < 0.05$ ). The comparison among both manual plans  $M_1$  and  $M_2$ , and computer-assisted plans  $C$  (Tables 2 and 3) revealed that the differences between  $M_1$  and  $C$  are on average  $0.5 \pm 0.5$  mm for diameter  $D$  and  $4.0 \pm 3.4$  mm for length  $L$  related to the pedicle screw size,  $1.6 \pm 1.1$  mm for pedicle crossing point  $p_c$ ,  $10.4 \pm 5.9^\circ$  for sagittal inclination  $\omega_x$  and  $5.8 \pm 4.1^\circ$  for axial inclination  $\omega_z$  related to the insertion trajectory, and  $16 \pm 20\%$  for normalized screw fastening strength  $F_n$ . The differences between  $M_2$  and  $C$  are on average  $0.4 \pm 0.3$  mm for diameter  $D$  and  $3.5 \pm 3.3$  mm for length  $L$  related to the pedicle screw size,  $1.5 \pm 1.1$  mm for pedicle crossing point  $p_c$ ,  $10.6 \pm 5.9^\circ$  for sagittal inclination  $\omega_x$  and  $4.6 \pm 3.6^\circ$  for axial inclination  $\omega_x$  related to the insertion trajectory, and  $19 \pm 22\%$  for normalized screw fastening strength  $F_n$ . Statistically significant differences were observed for planning of the pedicle screw size ( $p < 0.001$ ) and inclinations ( $p < 0.05$ ), where, in comparison to  $M_1$  and  $M_2$ , computer-assisted planning  $C$  did not propose narrower ( $p < 0.05$ ) and shorter ( $p < 0.001$ ) screws, but the corresponding normalized fastening strength was higher ( $p < 0.001$ ).

## 4 Discussion

In this paper, we present a quantitative comparison and analysis of manual and computer-assisted preoperative planning of the pedicle screw size and insertion trajectory. Although modern software enables 3D visualization of medical images, navigation through 3D images and manipulation with 3D pedicle screw models, the above described manual planning of the pedicle screw size and insertion trajectory is still a relatively time-consuming procedure. Moreover, by manual planning it is impossible to take into account all parameters, which are



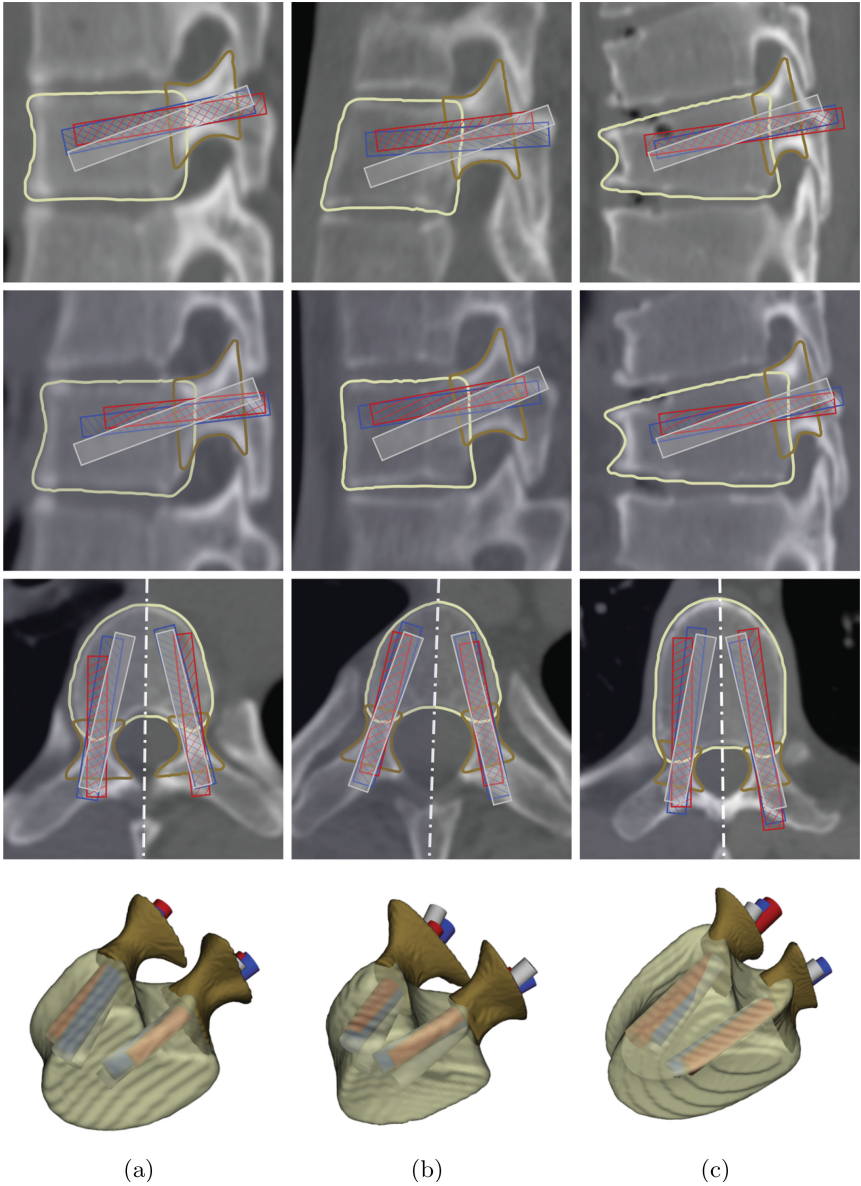


**Fig. 2.** Manual planning  $M_1$  (in red), manual planning  $M_2$  (in blue) and computer-assisted planning  $C$  (in gray) of the pedicle screw size and insertion trajectory for (a) patient 1: segment T7, (b) patient 4: segment T3 and (c) patient 12: segment T10. From top to bottom are displayed the sagittal CT cross-sectional view through the right pedicle, the sagittal CT cross-sectional view through the left pedicle, the axial CT cross-sectional view through both pedicles, and a 3D view. (Color figure online)



important for the insertion of pedicle screws, such as the screw pull-out strength and the corresponding screw fastening strength. On the other hand, computer-assisted planning is a relatively fast procedure, as it can be performed without the presence of a spine surgeon and/or a second observer, while still allowing to perform some eventual manual adjustments or other settings. An important advantage of computer-assisted planning is its repeatability and reliability, because it is based on the optimization of the parameters that are important for pedicle screw placement, i.e. searching for the highest possible screw fastening strength for the observed structure and shape of the vertebral body and pedicle.

The differences between manual plans ( $M_1$  vs.  $M_2$ ), obtained from two experienced spine surgeons, were on average relatively small, however, surgeon  $M_1$  proposed narrower and longer pedicle screws with a smaller corresponding normalized fastening strength. The size and the related fastening strength of manually planned pedicle screws are consistent with the findings of Chapman et al. [12] and Bianco et al. [13], who reported that the screw pull-out strength is mainly affected and in fact increases by its diameter. However, the pedicle screw length, compared to its diameter, does not largely affect its pull-out strength, which additionally confirms the findings of Hirano et al. [14], who reported that approximately 60% of the pedicle screw pull-out strength is within the pedicle and the remaining 40% is within the vertebral body. The differences between manual and computer-assisted plans ( $M_1$  vs. C and  $M_2$  vs. C) are comparable according to the order of magnitude, which is consistent with previous finding that the differences between both manual plans are relatively small. Furthermore, the average differences between both manual plans and computer-assisted plans ( $M_1$  vs. C and  $M_2$  vs. C) are in most cases relatively small and comparable to the differences between manual plans ( $M_1$  vs.  $M_2$ ), except for the sagittal inclination of the screw insertion trajectory, where on average higher differences occurred because vertebral morphometry allows a greater range of pedicle screw inclinations in the sagittal plane. As a result, two techniques of pedicle screw insertion are established in clinical practice, i.e. the anatomical technique with the screw insertion trajectory parallel to the longitudinal axis of the pedicle [15], and the straight-forward technique with the screw insertion trajectory parallel to the superior endplate of the vertebral body [16], where a difference of up to  $25^\circ$  in sagittal screw inclinations can occur between both insertion techniques [2]. The average differences in sagittal screw inclinations between the obtained manual and computer-assisted plans are within the above mentioned range (i.e.  $10.4 \pm 5.9^\circ$  for  $M_1$  vs. C and  $10.6 \pm 5.9^\circ$  for  $M_2$  vs. C), and the analysis of non-absolute differences in sagittal inclinations revealed that computer-assisted plans were more consistent with the anatomical technique, while manual plans were more consistent with the straight-forward technique. The statistical analysis of the obtained results also revealed that, at higher screw fastening strength, computer-assisted plans did not result in narrower and shorter pedicle screws when compared to both manual plans, which is in accordance to the above mentioned findings that the pedicle screw length does not largely influence the screw pull-out strength in comparison to the screw diameter.

**Acknowledgements.** This work was supported by the Slovenian Research Agency under grants P2-0232, J2-5473, J7-6781 and J2-7118. The authors thank Ekliptik d.o.o., Slovenia, for using EBS for manual preoperative pedicle screw placement planning.

## References

1. Tian, N.F., Huang, Q.S., Zhou, P., Zhou, Y., Wu, R.K., Lou, Y., Xu, H.Z.: Pedicle screw insertion accuracy with different assisted methods: a systematic review and meta-analysis of comparative studies. *Eur. Spine J.* **20**(6), 846–859 (2010)
2. Lehman, R.A., Polly, D.W., Kuklo, T.R., Cunningham, B., Kirk, K.L., Belmont, P.J.: Straight-forward versus anatomic trajectory technique of thoracic pedicle screw fixation: a biomechanical analysis. *Spine* **28**(18), 2058–2065 (2003)
3. Lee, C.S., Park, S.A., Hwang, C.J., Kim, D.J., Lee, W.J., Kim, Y.T., Lee, M.Y., Yoon, S.J., Lee, D.H.: A novel method of screw placement for extremely small thoracic pedicles in scoliosis. *Spine* **36**(16), E1112–E1116 (2011)
4. Koktekir, E., Ceylan, D., Tatarli, N., Karabagli, H., Recber, F., Akdemir, G.: Accuracy of fluoroscopically-assisted pedicle screw placement: analysis of 1,218 screws in 198 patients. *Spine J.* **14**(8), 1702–1708 (2014)
5. Cho, S.K., Skovrlj, B., Lu, Y., Caridi, J.M., Lenke, L.G.: The effect of increasing pedicle screw size on thoracic spinal canal dimensions: an anatomic study. *Spine* **39**(20), E1195–E1200 (2014)
6. Kleck, C.J., Cullimore, I., LaFleur, M., Lindley, E., Rentschler, M.E., Burger, E.L., Cain, C.M.J., Patel, V.V.: A new 3-dimensional method for measuring precision in surgical navigation and methods to optimize navigation accuracy. *Eur. Spine J.* **25**(6), 1764–1774 (2016)
7. Gstoettner, M., Lechner, R., Glodny, B., Thaler, M., Bach, C.M.: Inter- and intraobserver reliability assessment of computed tomographic 3D measurement of pedicles in scoliosis and size matching with pedicle screws. *Eur. Spine J.* **20**(10), 1771–1779 (2011)
8. Knez, D., Likar, B., Pernuš, F., Vrtovec, T.: Computer-assisted screw size and insertion trajectory planning for pedicle screw placement surgery. *IEEE Trans. Med. Imaging* **35**(6), 1420–1430 (2016)
9. Lee, J., Kim, S., Kim, Y.S., Chung, W.K.: Optimal surgical planning guidance for lumbar spinal fusion considering operational safety and vertebra-screw interface strength: optimal surgical planning guidance for lumbar spinal fusion. *Int. J. Med. Robot.* **8**(3), 261–272 (2012)
10. Schreiber, J.J.: Hounsfield units for assessing bone mineral density and strength: a tool for osteoporosis management. *J. Bone Jt. Surg. Am.* **93**(11), 1057–1063 (2011)
11. Linte, C.A., Augustine, K.E., Camp, J.J., Robb, R.A., Holmes III, D.R.: Toward virtual modeling and templating for enhanced spine surgery planning. In: Li, S., Yao, J. (eds.) *Spinal Imaging and Image Analysis*. LNCVB, vol. 18, pp. 441–467. Springer, Cham (2015)
12. Chapman, J.R., Harrington, R.M., Lee, K.M., Anderson, P.A., Tencer, A.F., Kowalski, D.: Factors affecting the pullout strength of cancellous bone screws. *J. Biomech. Eng.* **118**(3), 391–398 (1996)
13. Bianco, R.J., Arnoux, P.J., Wagnac, E., Mac-Thiong, J.M., Aubin, C.É.: Minimizing pedicle screw pullout risks: a detailed biomechanical analysis of screw design and placement. *J. Spinal Disord. Tech.* (2014). Publish Ahead of Print <https://www.ncbi.nlm.nih.gov/pubmed/25075993>

14. Hirano, T., Hasegawa, K., Takahashi, H.E., Uchiyama, S., Hara, T., Washio, T., Sugiura, T., Yokaichiya, M., Ikeda, M.: Structural characteristics of the pedicle and its role in screw stability. *Spine* **22**(21), 2504–2509 (1997)
15. Weinstein, J.N., Rydevik, B.L., Rauschnig, W.: Anatomic and technical considerations of pedicle screw fixation. *Clin. Orthop.* **284**, 34–46 (1992)
16. Roy-Camille, R., Saillant, G., Mazel, C.: Internal fixation of the lumbar spine with pedicle screw plating. *Clin. Orthop.* **203**, 7–17 (1986)